

ACTIVE FLUORIDE GLASSES

Paweł Szczepański

Some properties of the active fluoride glasses are discussed. Glass composition and fabrication techniques are presented. Fluorescence transitions of rare earth in fluoride glasses are shown, which reveal a wide range of potential applications of this kind of glasses in telecommunication systems, optoelectronics and medicine. A material and device study for obtaining upconversion fibre laser in visible spectrum range is presented in detail.

INTRODUCTION

Fluoride glasses based on zirconium fluoride (fluorozirconates) were initially discovered at the University of Rennes, in France in 1974 [1]. Other fluoride systems had been known but were highly toxic (BeF_2) or very unstable (AlF_3), and this was the first fluoride system that was essentially practical to use. It made possible to developed technology of the fluoride glasses.

Preparation of these glasses occurs straight forward and the resulting samples exhibit a wide range transparency, extending from about $0.2\mu\text{m}$ - $7\mu\text{m}$. This characteristics, along with an index of refraction near 1.5 and good resistance to degradation from water or weak acids makes these materials promising candidates for optical fibre [2]. Especially, a very good infrared transmitting properties make the intriguing losses of these glasses significantly below those in silica and fluoride glasses are now being investigated for use in ultra-low-loss fibres [3].

The composition of the glasses is such that the trivalent lanthanides are easily incorporated, which makes these glasses good laser hosts. The first fluoride fibre laser was demonstrated at $1.05\mu\text{m}$ using Nd as a dopant [4]. Follo-

wing this work many new dopants have been investigated and many lasing lines have been reported. In particularly studies on the optical properties of rare-earth ions in fluoride glasses have been on Nd^{3+} [5], Eu^{3+} [6], Er^{3+} [7-11], Tm^{3+} [12,13], Pr^{3+} [14], Ho^{3+} [15,16]. Fluoride fibre lasers using Er^{3+} [17-26], Nd^{3+} [4], Tm^{3+} [27-32], Pr^{3+} [33-35], and Ho^{3+} [36-38] have been demonstrated. Moreover, fibre amplifiers have been presented at $0.8\mu\text{m}$ [39,40], $1.5\mu\text{m}$ [51-59], $1.3\mu\text{m}$ [41-50] and $2.7\mu\text{m}$ [78].

It is worth noting that the latter two wavelengths are especially significant since they are as yet unavailable in silica based fibre. This fact is mainly caused by the low phonon energies (500cm^{-1}) of the fluoride glass, hosts in comparison with silica glasses, which reduce nonradiative transitions due to multiphonon emission. The relatively low phonon energies also help in obtaining an up-conversion effects in these active glasses leading, for example, to green and blue light emission [60-67].

In this paper we describe some properties of the active fluoride glasses and their possible applications. In Sec.II the fluoride glasses as laser host materials are presented. Glass composition and fabrication techniques are discussed. In Sec.III fluorescence transitions of rare earth in ZBLAN are shown. In the next section a material and device study for obtaining upconversion fibre laser in visible spectrum range is presented. Sec.V gives conclusions.

FLUORIDE GLASSES AS LASER HOST MATERIALS

In this section we describe some material properties of the fluoride glasses and methods of fabrication.

GLASS COMPOSITION

The most stable composition among different fluorozirconate compositions investigated up to date, especially for fibre drawing, is $\text{ZrF}_4\text{-BaF}_2\text{-LaF}_3\text{-AlF}_3\text{-NaF}$ so called ZBLAN for short. The index of the glass is about 1.5, and the melting temperatures are in the range $500\text{-}700^\circ\text{C}$. In the case of the fibres, an index difference between the core and cladding glasses can be achieved, for example, by adding PbF_2 to the core or HfF_4 to the cladding [2].

In general the structure of the ZBLAN is not very well understood. Ac-

According to [68] the Zr and Al are thought to be network formers, La to be an intermediate (can play a role of former). In general fluoride glasses consist of heavy elements. This results in the fundamental phonon energies lying at longer wavelengths (525cm^{-1}) than silicates [68,69]. Besides leading to low intrinsic losses, this property leads also to lower non-radiative decay rates, causing higher quantum efficiencies than many other glass systems, see Fig.1.

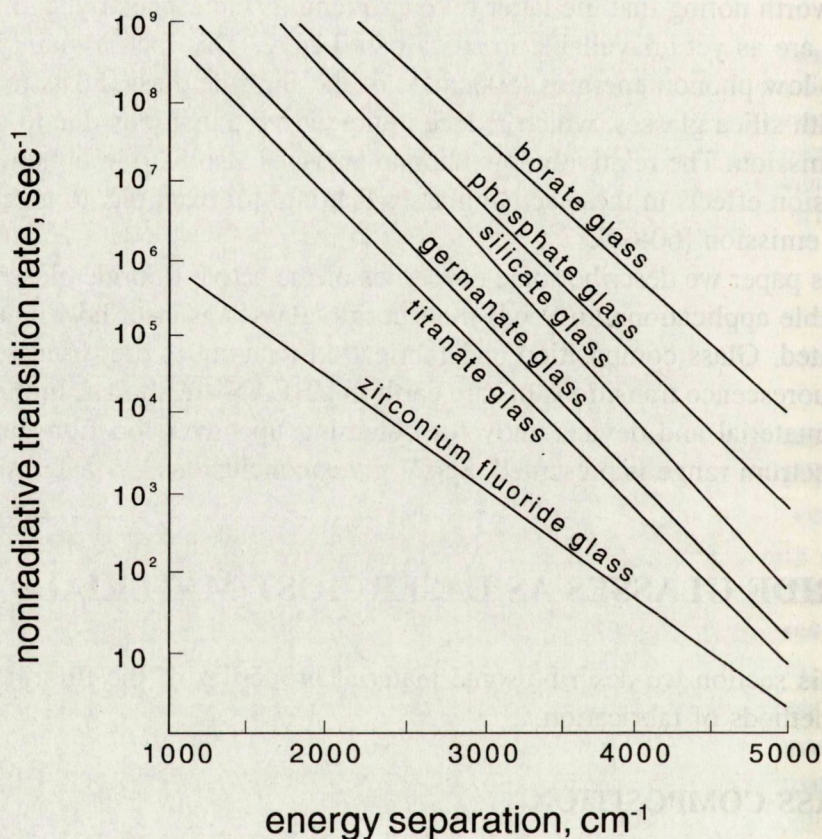


Fig. 1 Non-radiative decay rates for several glasses (after [69]).

On further point is that fluoride glasses will exhibit many more fluorescing transitions than other hosts. A good example is the fluorescence spectrum of Ho^{3+} in ZBLAN which exhibits several bands that are not observed in silica. Moreover for many levels the lifetimes in fluoride glasses will be longer than in other glasses. Besides the possibility of lower thresholds for

lazing, this also offers the possibility for up-conversion. The longer lifetimes allow a greater probability for two-photon (or more) absorption as well as for an excited-state absorption (ESA), required for up-conversion lasers. However, the latter effect on the other hand can be detrimental property in the case of some fibre amplifier systems. For example, the emission cross section of Nd close to $1.3\mu\text{m}$ is reduced by signal excited-state absorption. [70].

FABRICATION TECHNIQUES

The most successful fibre-drawing techniques for fluoride glasses is the preform process, whereby glass melts are converted into preforms which are finally drawn into optic fiber. The most stable glasses so far discovered are based on ZBLAN. Thus this glass is the most favoured for fibre making. The list of some popular compositions is given in Table 5. The constituents are given in mol%.

Glass melting and preform fabrication

The starting materials are in general anhydrous fluorides stored in glove boxes to prevent hydrolysis. The melting crucibles are usually either vitreous carbon or Pt/Au. A typical melting schedule includes an initial hold at 400°C to allow fluoridation, followed by a rise in temperature to 850°C to allow fusion and melting. Oxygen can be introduced in order to oxidise the melt. The melt is then cooled to 670°C prior to casting in a brass mould.

The casting technique [73] is based on an old-established method used in other systems to form tubes by rotational casting. In this case the mould is only partially filled with molten cladding glass, and the swung to a horizontal position and spun until the glass cools to form a tube. In this way controlled cladding tubes can be fabricated and the core glass is then cast into this tube. A small lathe is used for spinning the mould and the typical spin speed is 5000 r.p.m. The moulds are often fabricated in brass, although some authors have suggested gold coating, and are split along the central - line for easy removal of the preform. After casting the mould is transferred into a separate annealing oven situated below the glove box, again without coming into contact with ambient. Since the outer surface of the molten glass is brought into contact a potentially contaminating metal during the casting process, several

techniques have been developed to remove the outer layer from the preform. They include mechanical polishing and chemical etching and the techniques are able to improve both the fibre strength and the loss.

Fibre drawing

The techniques used to draw preforms into fibre are based on standard methods developed for silica fibre. The main difference is the draw furnace since much lower temperatures are required for fluoride fibres. A feeder is used to lower the preform into the furnace at constant rate. The preform is mounted inside a silica liner which is sealed at the top end around the stainless steel rod so that dry nitrogen can be flushed through the chamber. In this way surface crystallisation during reheating of the preform to draw fibre can be kept to a minimum. A diameter monitor is used to measure the fibre diameter, and the output from the monitor is then servo-linked to the winding drum speed controller. In this way the diameter is controlled to 2mm. Polymer coatings cured by UV light can be applied in the usual way. Essentially, epoxy acrylates can be applied in the liquid.

FLUORESCENCE TRANSITIONS OF RARE EARTH IN ZBLAN

For laser action, among other features, there must be a strong fluorescence at required wavelength. Fluorescence spectra of rare-earth ions in the glass host are therefore very useful firstly to identify possible pump-bands and secondly in identifying possible lasing wavelength.

A comprehensive set of emission spectra of lanthanides in a ZBLAN host has been given in [71]. A list of peak emission wavelengths and assigned transitions is given in Table 1. and 2, made by reference to the rare-earth ion energy diagram given in Fig.2. Emissions are observed over the whole range 0.5-3.0 μm , offering the possibility of an extensive set of lasing emissions, confirming that the ZBLAN host has a relatively high radiative efficiency.

Table 1. Fluorescence transitions of rare earths in ZBLAN. Transitions and related wavelength [μm] peaks are shown.

Pr	Nd	Sm	Eu	Tb
$3P_0 \rightarrow 3H_6$ 0.603	$4F_{3/2} \rightarrow 4I_{9/2}$ 0.867	$4G_{5/2} \rightarrow 6H_{5/2}$ 0.560	$5D_0 \rightarrow 7F_1$ 0.591	$5D_4 \rightarrow 7F_5$ 0.543
$3P_0 \rightarrow 3F_2$ 0.635	$4F_{3/2} \rightarrow 4I_{11/2}$ 1.048	$4G_{5/2} \rightarrow 6H_{7/2}$ 0.595	$5D_0 \rightarrow 7F_2$ 0.615	$5D_4 \rightarrow 7F_4$ 0.585
$1D_2 \rightarrow 3H_5$ 0.695	$4F_{3/2} \rightarrow 4I_{13/2}$ 1.318	$4G_{5/2} \rightarrow 6H_{9/2}$ 0.641	$5D_0 \rightarrow 7F_4$ 0.698	$5D_4 \rightarrow 7F_3$ 0.585
$3P_0 \rightarrow 3F_4$ 0.717	$4F_{3/2} \rightarrow 4I_{13/2}$ 1.945	$4G_{5/2} \rightarrow 6H_{11/2}$ 0.704		$5D_4 \rightarrow 7F_2$ 0.585
$3P_0 \rightarrow 1G_4$ 0.908		$4G_{5/2} \rightarrow 6H_{13/2}$ 0.782		$5D_4 \rightarrow 7F_1$ 0.668
$1D_2 \rightarrow 3F_4$ 1.014		$4G_{5/2} \rightarrow 6H_{15/2}$ 0.896		$5D_4 \rightarrow 7F_0$ 0.681
$1G_4 \rightarrow 3H_5$ $1D_2 \rightarrow 1G_4$ 1.326 1.406		$4G_{5/2} \rightarrow 6F_{5/2}$ 0.936		
$1G_4 \rightarrow 3F_2$ $3H_6 \rightarrow 3H_4$ 2.300		$4G_{5/2} \rightarrow 6F_{7/2}$ 1.022		
		$4G_{5/2} \rightarrow 6F_{9/2}$ 1.162		
		$4G_{5/2} \rightarrow 6F_{11}$ 1.376		

Table 2. Fluorescence transitions of rare earths in ZBLAN. Transitions and related wavelength [μm] peaks are shown.

Dy	Ho	Er	Tm	Yb
$4F_{9/2} \rightarrow 6H_{13/2}$ 0.575	$5S_2 \rightarrow 5I_8$ 0.543	$5S_2 \rightarrow 4I_{15/2}$ 0.543	$1G_4 \rightarrow 3F_4$ 0.694	$2F_{5/2} \rightarrow 2F_{7/2}$ 1.0
$4F_{9/2} \rightarrow 6H_{11/2}$ 0.661	$5S_2 \rightarrow 5I_7$	$4F_{9/2} \rightarrow 4I_{15/2}$	$1G_4 \rightarrow 3H_5$ $3H_4 \rightarrow 3H_6$ 0.799	
$4F_{9/2} \rightarrow 6H_{9/2}$ $4F_{9/2} \rightarrow 6F_{11/2}$ 0.750	$5S_2 \rightarrow 5I_6$ 1.015	$4S_{5/2} \rightarrow 4I_{13/7}$ 0.847	$1G_4 \rightarrow 3H_5$ $3F_3 \rightarrow 3F_4$ $3H_5 \rightarrow 3H_6$	
$4F_{9/2} \rightarrow 6H_{7/2}$ $4F_{9/2} \rightarrow 6F_{9/2}$ 0.834	$5I_6 \rightarrow 5I_8$ 1.154	$4I_{11/2} \rightarrow 4I_{15/2}$ 0.997	1.184 $1G_4 \rightarrow 3F_3$ $3H_4 \rightarrow 3F_4$	
$4F_{9/2} \rightarrow 6H_{5/2}$ 0.924	$5I_6 \rightarrow 5I_8$ 1.191	$4S_{3/2} \rightarrow 4I_{11/7}$ 1.219	1.464 $2F_4 \rightarrow 3H_6$	
$4F_{9/2} \rightarrow 6F_{5/2}$ 1.0	$5S_2 \rightarrow 5I_5$ 1.381	$4I_{13/2} \rightarrow 4I_{15/2}$ 1.538	1.847 $3H_4 \rightarrow 3H_5$	
$4F_{9/2} \rightarrow 6F_{5/2}$ 1.170	$5S_2 \rightarrow 5I_4$ 1.953	$4I_{11/2} \rightarrow 4I_{13/2}$ 2.719	2.307	
$4F_{9/2} \rightarrow 6F_3/2$ 1.294	$5I_7 \rightarrow 5I_8$ 2.039			
$4F_{9/2} \rightarrow 6F_{12}$ 1.384	$5I_6 \rightarrow 5I_7$ 2.848			

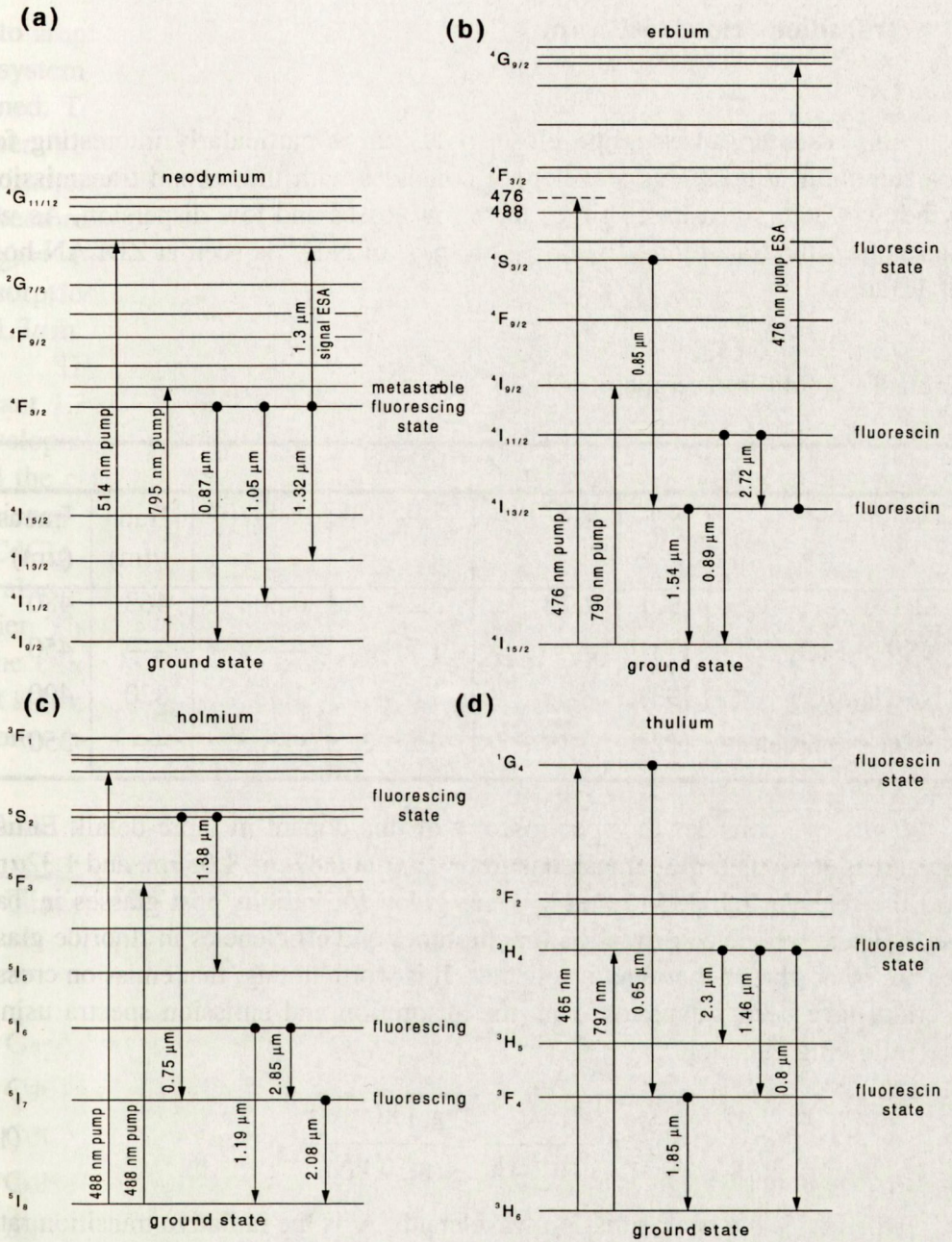


Fig. 2 Energy diagrams for Nd^{3+} , Er^{3+} , Ho^{3+} , and Tm^{3+} in ZBLAN, (after [92]).

Transitions close to 1.3 μm

In particular, an emission close to 1.3 μm is particularly interesting for telecommunications. This wavelength coincides with the second transmission window where silica-based fibres have low losses and low dispersion. As we can notice, the transition ${}^4\text{F}_{13/2} \rightarrow {}^4\text{I}_{13/2}$ of Nd^{3+} is seen at ZBLAN host at 1.32 μm .

Table 3. Nd^{3+} in several hosts.

Host class	Ref.	$\sigma_p \times 10^{20} \text{cm}^2$			τ_{rad} (μs)	τ_{meas} (μs)
		0.87 μm	1.05 μm	1.32 μm		
ZBLAN	[93]	1.23	3.29	0.60	463	480
NS918(SiO_2)	[73]	—	1.7	—	—	450
Na-Ca- SiO_2	[93]	—	1.65	1.35	820	400
LHG-8 (phosphate)	[72]	—	4.2	—	—	350

Thus, we consider the spectroscopy of this dopant in more detail. Emission cross-sections for the transitions from ${}^4\text{F}_{13/2}$ at 0.87 μm , 1.05 μm , and 1.32 μm and the relevant radiation times τ_{rad} are given for various host glasses in Table.3. There we see confirmation that lifetimes and efficiencies in fluoride glasses are somewhat higher than in silicates. It is worth noting, that emission cross-section have been calculated from the absorption and emission spectra using the following equation

$$\sigma_p = \frac{\lambda_p^2 A_r}{8 \pi n^2 \Delta \nu} = \frac{g_i \int k(\nu) d \nu}{g_j \Delta \nu N_0}, \quad (1)$$

where λ_p is the peak emission wavelength, A_r is the radiative transition rate for the given transition, $\Delta \nu$ is the effective emission linewidth, g_i and g_j are the initial and final state degeneracies, $k(\nu)$ is the absorption coefficient and N_0 is the concentration of dopant ions.

Another dopant, which has recently received attention owing to its ability

to amplify a signal in the $1.3 \mu\text{m}$ window is praseodymium [74,75]. For fiber system based on ZBLAN:Pr³⁺ net gains of more than 10 dB have been obtained. To optimise the amplifier, it may be useful to use a codopant as sensitiser. Ytterbium has been extensively studied as sensitiser in energy transfer experiments [76]. However recently, an energy transfer between Yb³⁺ and Pr³⁺ has been reported [77]. It has been shown the energy transfer Yb³⁺ ($^2F_{7/2} \rightarrow ^2F_{5/2}$) \Rightarrow Pr³⁺ ($^3H_2 \rightarrow ^1G_4$) offers for pumping between $0.85 - 1 \mu\text{m}$ in the absorption band of Yb³⁺ possibility to obtain higher amplifier efficiency for $1.3 \mu\text{m}$.

The maximalization of the quantum-efficiency in the commercially important $1.3 \mu\text{m}$ optical fibre amplifiers caused also an immense interest of the development of glasses which offer possible low maximal phonon energy. In Table 4 the comparison of the radiative and nonradiative lifetimes and quantum efficiency for 1G_4 of Pr³⁺ in various glasses is shown [78]. The Ga₂S₃:La₂S₃, CdCl₂ and CdCl₂:CdF₂ glass systems offer quantum efficiency above 25% a value which is considered to be the minimum for viable $1.3 \mu\text{m}$ optical amplifier. The Ga₂S₃:La₂S₃ glass is thermally and environmentally more stable than the chloride-based glasses, which have relatively poor resistance to moisture. It shows intrinsic losses in the 1mm less than 0.1dB/m and has the potential to form the low-loss optical fibres.

Table 4. Radiative and nonradiative lifetimes for 1G_4 level of Pr³⁺

Glass	Radiative lifetime	Noradiative lifetime	Total lifetime*	Theoretical QE**	Measured QE**
	ms	ms	ms	%	%
Ga ₂ S ₃ :La ₂ S ₃	700	8440	650	93	26
CdCl ₂	2460	3950	1520	62	3
CdCl ₂ :CdF ₂	2460	1020	721	29	4
CdF ₂	3210	1020	774	24	6
InF ₃	4730	270	255	5	5
HfF ₄	3210	110	106	3	4
ZrF ₄	3200	120	116	4	4
TeO ₂ -ZnCl ₂	1800	8	8	0.4	—

*) Total lifetime = $\tau_{\text{rad}} \tau_{\text{nrad}} / (\tau_{\text{rad}} + \tau_{\text{nrad}})$

***) QE - quantum efficiency

However, this glass has the peak wavelength of the $1.3\mu\text{m}$ emission shifted away from the second telecommunications window.

Transitions close to $1.5\mu\text{m}$

Another line, very interesting for telecommunication applications is the wavelength $\lambda = 1.54\mu\text{m}$. This wavelength is offered by the ${}^4I_{13/2} \rightarrow {}^4I_{15/2}$ transition in Er^{3+} . This line is observed in silica-based fibres but it also exists as expected in ZBLAN. The comparison between the emission cross-section and the radiation lifetime for the ZBLAN and the silica host is given in Table 5. In ZBLAN the optimum pump wavelength is likely to be 1495 nm rather than 1480 nm as in the case of silica.

Table 5. Er^{3+} in several hos glasses.

Host glass	Ref.	$s_p \times 10^{20} \text{ cm}^2$	t_{rad} (ms)	t_{meas} (ms)
ZBLAN	[93]	0.47	11	11
ZBLAN	[94]	0.63	-	-
Al-P-SiO ₂	[94]	0.55	10	10

Transitions in range $2\text{-}3.5\mu\text{m}$

Laser sources in the region $2\text{-}3\mu\text{m}$ are currently being investigated with a view to application in such diverse fields as telecommunications, medicine, eye safe radar and remote sensing. In pursuit of efficient, compact, and cheap sources of laser radiation much more interest is now being focused on rear-earth doped fluoride fibre systems as opposed to the more traditional rare-earth silica glass fibres.

In particular, there is a requirement for parallel programmes of work investigating the feasibility of receivers and transmitters for operation at the predicted low loss minimum wavelength $2.25\mu\text{m}$. Rare earth doped fluoride fibre

lasers offer many advantages as a transmitters and in line optical amplifiers in this application. Narrow linewidths would ensure minimum dispersion penalty in long span systems, and broadband tuneability could be employed to attain an exact match between lasing wavelength and the minimum loss wavelength $2.25\mu\text{m}$.

The concept has been already explored in some detail with work concentrating on the erbium transition centred at $2.7\mu\text{m}$. [78]. Unfortunately the short wavelength tail of the OH absorption peak at $2.87\mu\text{m}$ gives a predicted background loss at this wavelength of 0.5dB/km/ppb . For practical fibre laser sources thulium doping seems to be more desirable option. The tuneable laser emission in the $2.27\text{-}2.4\mu\text{m}$ [30] in ZBLAN:Tm³⁺. In this case the losses due to the OH absorption are negligible ($<0.025\text{dB/km/ppb}$).

An interesting mechanism for obtaining near theoretical maximum slope efficiency at $1.925\mu\text{m}$ has been obtained by forcing simultaneous operation of $1.82\mu\text{m}$ and $2.32\mu\text{m}$ transitions in Tm-doped ZBLAN [79]. These transitions previously inhibited each other, can be operated simultaneously.

The laser operation at wavelength $2\mu\text{m}$ is very interesting because of the strong potential applications in medicine. Such a transition has been observed in holmium doped ZBLAN [15,16]. An inability to demonstrate efficient performance [15,16] could be attributed to the lack of a suitable absorption band in the near infra-red which could be pumped by commercially available semiconductor lasers. More recently, this problem has been solved by using Tm as a codopant [80]. Pumping of the holmium laser through thulium offers a higher pump quantum efficiency due to the cross-relaxation process. For this case the slope efficiency of 60% of the laser operation at $2.04\mu\text{m}$ has been observed by pumping into the thulium absorption band between 820 and 830 nm.

HIGH BRIGHTNESS BLUE AND GREEN LIGHT SOURCES

An immense interest of the development of the compact blue coherent light sources is caused by the high density optical recording (HDOR), where data storage capacity increases with the decreasing recording wavelength. On the other hand the green coherent light sources are sought for because of the applications in underwater telecommunications systems and underwater pollution

monitoring.

In general, several possible ways to construct a compact coherent source generating in the visible range of the optical spectrum are possible. Most efforts deal with second harmonic generation (SHG) to convert infrared laser diode light into blue laser light. The most important disadvantage of SHG is the phase matching condition. It requires a strict control of the temperatures of both the SHG material and the laser diode and an accurately defined pumping wavelength of the laser diode.

Another process used to convert laser diode light into blue or green light is based on the upconversion effect. This process has the disadvantage spontaneous blue (green) light is generated whereas SHG results in laser light. This means that, in order to obtain blue laser light, upconversion has to take place into a laser resonator cavity, a condition which is not required for SHG. Moreover, the laser diodes at about 650nm are required as a pumping source (high power laser diodes at 800nm are further ahead in their development than the red laser diodes). On the other hand, a major advantage of the upconversion is that no severe demands for temperature control and excitation wavelength are necessary.

The upconversion process

Upconversion is a process which converts long-wave radiation into shortwave radiation by multiphoton mechanism. In the case of rare earth ions, energies of the absorbed photons are added into the energy levels scheme, resulting in the population of higher excited state than can be accomplished by one-photon absorption. Subsequent emission from the higher excited state yields photons with higher energy than of the absorbed photons.

Two different upconversion processes can be discerned as shown in Fig.3. In the case of the excited state absorption (ESA) process, addition of the photon energies is a result of the absorption of the another photon while the rare earth ion is in an excited state (state 1 in Fig.3). In the other case addition of photon energies occurs by energy transfer between two adjacent rare earth ions in excited state 1 resulting in one rare earth ion in state 2 and the other in the ground state (state 0). This process is called APTE (addition of photons by energy transfer). In general APTE process is more efficient than ASE process and it depends on the rare earth concentration.

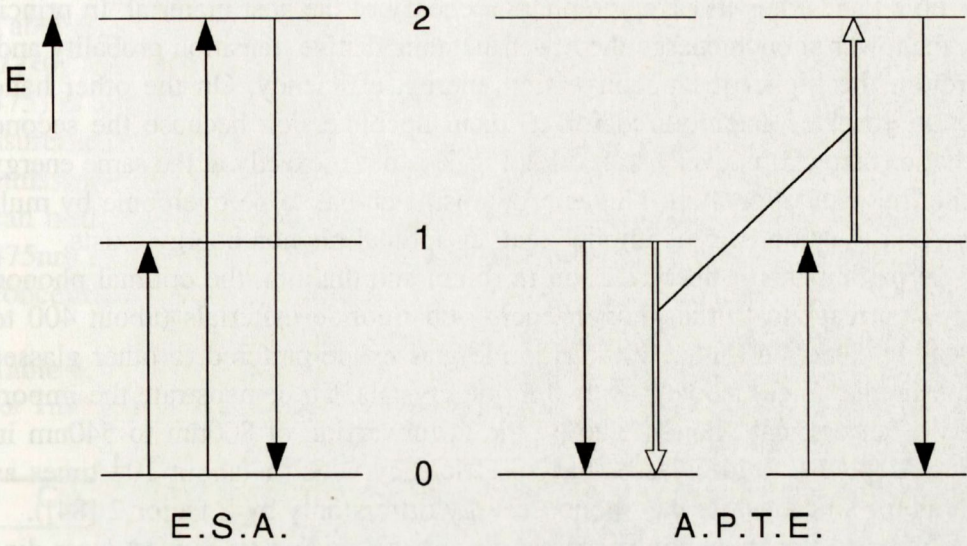


Fig. 3 Schematic representations of the ESA (excited state absorption) and EPTE (addition of photons by energy transfer) upconversion processes.

For the upconversion process in which n (long-wave) photons are converted into one (short-wave) photon it is found that [81]

$$P_{out} = \eta (P_{abs})^n, \quad (2)$$

where P_{abs} is the absorbed input power and η is a constant depending on the kind of upconversion process. For two-photon process the overall upconversion efficiency (P_{out}/P_{abs}) varies linearly with the input power. The upconversion efficiency also depends strongly on the rare earth concentration and on the host materials. Too high a rare earth concentration will result in efficient cross-relaxation process [82] (inverse to APTE). Because the efficiency of the APTE process also increases with the rare earth concentration this implies that there exists an optimal rare earth concentration for efficient upconversion efficiency.

Nonradiative processes also seriously decrease the upconversion efficiency. The probability for a nonradiative transition - P_{NR} , is given by [83]

$$P_{NR} = C \exp(-\Delta E/\eta n), \quad (3)$$

where ΔE is the energy difference between the subsequent energy levels

concerned and $\eta\nu$ is the average phonon energy of the host material. In principle, the lower phonon energy the lower the nonradiative transition probability and, therefore the higher the upconversion energy efficiency. On the other hand phonon energies are required for efficient upconversion because the second excitation step (from level 1 to level 2, Fig.3) is never exactly at the same energy as the first excitation step. This energy mismatch has to be overcome by multi-phonon transitions. This implies that an optimal phonon energy exists.

In particular, for upconversion in erbium and thulium, the optimal phonon energy correspond to the phonon energy of fluoride materials (about 400 to 500 cm^{-1}). Thus, in this case the fluoride glasses are preferred to other glasses (for example silica) as well as to fluoride crystals. To demonstrate the importance of an optimal phonon energy: the upconversion of 800nm to 540nm in erbium doped fluoride glasses has an efficiency which is about 10^4 times as high as for silica (while the phonon energy differs only by a factor 2 [84]).

Different upconversion processes have been studied to convert laser diode into light of a shorter wavelength. The conversion of 800nm into green light in erbium doped fluoride glasses [84-86] or upconversion of 650nm into green light in holmium doped fluoride glasses [87] have been demonstrated.

The only way to obtain blue light is upconversion process is by upconversion in thulium doped fluoride glasses. Thulium doped glasses codoped with ytterbium are suitable to convert 980nm light into blue light 475nm [88,89]. However, because of the three-step upconversion process the efficiency is not very high.

More promising upconversion process in thulium doped fluoride glass in order to obtain an efficient blue emitting device converting, a conversion process 650nm into 450nm light has been proposed [90-93]. In the next section we described this process in more details.

Blue upconversion in Tm^{3+} doped fluoride glasses

The blue part of the upconversion emission spectrum of a ZBLAN glass doped with 0.1 mol.% Tm^{3+} excited at 650 nm consists of two peaks; the band around 450 nm ($^1\text{D}_2 \rightarrow ^3\text{H}_4$) and the weaker transition around 480 nm ($^1\text{D}_4 \rightarrow ^3\text{H}_6$) [90,91]. the intensity ration of these bands with the excitation wavelength.

Tabel 6 [92] shows emission intensities of the blue emission bands at 450nm (I_{450}) and 475nm (I_{475}). C_{Tm} denotes the thulium concentration and $R(450/475)$ is the intensity ratio between the 450 and 475nm emission band. All measurements are performed for 647nm excitation under equal conditions, and the emission intensity for ZBLAN-Tm(0.1) is set to 100 (arbitrary units). As we can notice, the upconversion efficiency and the intensity ratio of the 450 and 475nm emission bands decrease for increasing Tm^{3+} concentrations. For Tm^{3+} concentration above 0.2mol.% this decrease is drastic.

Table 6. Integrated emission intensities of the blue emission bands at 450nm 475nm for Tm^{3+} doped ZBLAN. The emission intensity for ZBLAN-Tm(0.1) is set to 100 (a.u).

$C_{Tm}(\text{mol.}\%)$	$R(450/475)$	I_{450}	I_{475}
0.05	1.2 ± 0.1	49 ± 3	19 ± 2
0.1	2.4 ± 0.1	100 ± 2	46 ± 2
0.2	1.8 ± 0.1	296 ± 10	164 ± 10
0.5	1.2 ± 0.2	600 ± 50	490 ± 40
1	1.2 ± 0.1	1090 ± 30	850 ± 20

In general, the CW laser action at 450nm is hampered by the fact that lifetime of the lower level (6ms), state 3H_4 - Fig.4, is longer than the lifetime of the upper level (55ms), state 1D_2 . In the case an inversion of the population, necessary for laser action, is very difficult to obtained. Thus, the lifetime of the 3H_4 has to be shortened considerably. This can be achieved in several ways. In principle it is possible to quench the lifetime of the 3H_4 by using the upconversion process populating the 1G_4 state. In this case high excitation densities at the maximum excitation wavelength for this transition are required for efficient depopulation of the 3H_4 state. Another way to shorten the 3H_4 lifetime is by making the transition $^3H_4 \rightarrow ^3H_6$ lase simultaneously with the $^1D_2 \rightarrow ^3H_4$ transition. This will help to shorten the 3H_4 to some extent.

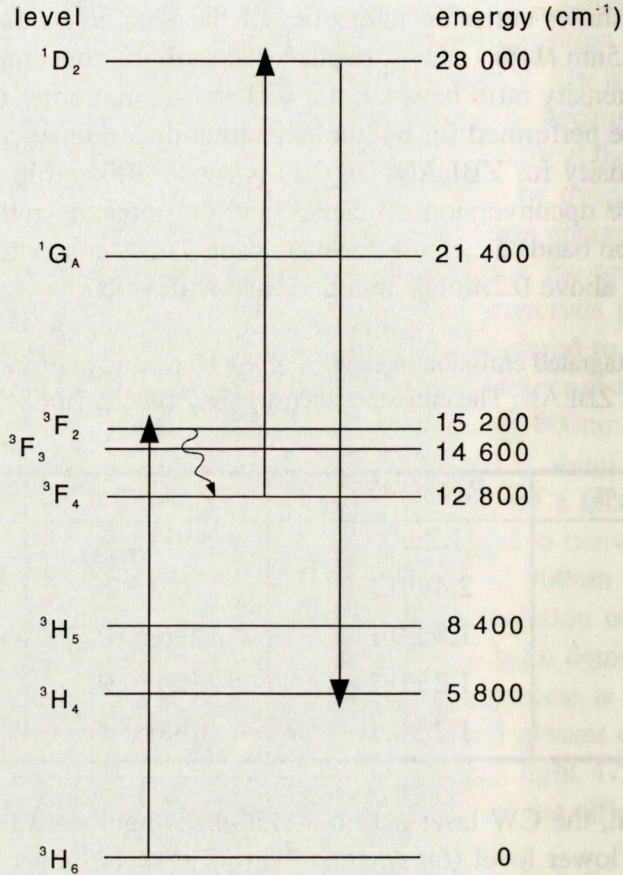


Fig. 4 Upconversion of 650 nm into 450 nm in Tm^{3+} .

It is also possible to quench the ${}^3\text{H}_4$ lifetime by co-doping the Tm^{3+} doped fluoride glass with a co-dopant which absorbs the excitation energy of Tm^{3+} in the ${}^3\text{H}_4$ state. In this way efficient quenching of the ${}^3\text{H}_4$ state can be obtained as a result of the energy-transfer from $\text{Tm}({}^3\text{H}_4)$ to the co-dopant. However, in this case a co-dopant must fulfil the following conditions:

- A strong absorption occurs at $1.7\mu\text{m}$ (it corresponds to the energy of the ${}^3\text{H}_4$ state). Preferably, this absorption results in populated levels of the co-dopant with a short lifetime

- Radiation at about 360, 450, 650, and 800nm is not, or is only weakly, absorbed.

Table 7. The intensity of the thulium emission at 450nm ($^1D_2 \rightarrow ^3H_4$), 475 nm ($^1G_4 \rightarrow ^3H_6$), 790 nm ($^3F_4 \rightarrow ^3H_6$) and 1600 nm ($^3H_4 \rightarrow ^3H_6$) for several Tm, Tb codoped samples upon 675nm excitation. The intensity of the sample without co-dopant is set to 100.

Dopant	I(450)	I(475)	I(790)	I(1600)	R(450/475)
Tm(0.1)	100±5	100±5	100±5	100±5	4.5±0.5
Tm(0.1)Tb(0.01)	85±5	70±7	89±5	96±5	5.3±0.5
Tm(0.1)Tb(0.1)	71±5	354	65±5	7753	9±1
Tm(0.1)Tb(1.4)	17±2	4±2	13±2	13±2	17±5
Tm(0.2)	100±5	100±5	100±5	100±5	3.7±0.5
Tm(0.2)Tb(0.01)	65±5	52±4	75±5	61±5	4.70.5
Tm(0.2)Tb(0.05)	55±5	37±4	68±5	56±5	55.810.6
Tm(0.2)Tb(0.4)	31±3	7±1	27±3	12±2	16±2
Tm(0.2)Tb(2.8)	4±1	0.5±0.5	4±1	3±2	≤40

In Tables 7-9 the effects of several co-dopands are shown. In general, Tb^{3+} seems to be the most suitable co-dopand to shorten lifetime $Tm(^3H_4)$ excited state while maintaining an efficient upconversion process of 650nm into blue light within Tm^{3+} ion. However Tb^{3+} also decreases the upconversion efficiency. The only way to limit this decrease in upconversion efficiency is by using high excitation densities at 650nm and using appropriate additional co-dopant.

Table 10 lists the properties of three laser fiber devices. All the lasers were made of ZBLAN glass and their cores were doped with respectively Tm^{3+} , Ho^{3+} and Er^{3+} . Above threshold, the outputs of all three fiber lasers were found to vary linearly. However, these devices have not been optimized with the respect to fiber parameters such as the dopant concentration.

Table 8. The intensity of the thulium emission at 450nm ($^1D_2 \rightarrow ^3H_4$), 475 nm ($^1G_4 \rightarrow ^3H_6$), 790nm ($^3F_4 \rightarrow ^3H_6$) and 1600 nm ($^3H_4 \rightarrow ^3H_6$) for several Tm, Pr, ;Tm,Sm and Tm,Dy co-doped samples upon 675 nm excitation. The intensity of the sample without co-dopant is set to 100.

Dopant	I(450)	I(475)	I(790)	I(1600)	R(450/475)
Tm(0.1)	100±5	100±5	100±5	100±5	4.6±0.5
Tm(0.1)Pr(0.1)	42±3	21±3	42±3	52±5	5.3±0.5
Tm(0.1)Pr(0.4)	14±1	6±1	14±2	17±3	10±1
Tm(0.2)	100±5	100±5	100±5	100±5	3.7±0.5
Tm(0.2)Pr(0.02)	49±3	37±3	56±3	56±3	4.9±0.5
Tm(0.2)Pr(0.1)	37±3	19±2	52±3	48±3	7.5±1
Tm(0.2)Pr(0.4)	6	2±1	19±2	16±2	10±1
Tm(0.2)	100±5	100±5	100±5	100±5	3.7±0.5
Tm(0.2)Sm(0.1)	40±3	37±3	49±3	56±3	4.0±0.5
Tm(0.2)Sm(0.5)	14±1	14±2	17±2	27±3	3.7±0.5
Tm(0.2)	100±5	100±5	100±5	100±5	3.7±0.5
Tm(0.2)Dy(1)	7±1	0.7±0.3	9±2	<5	30±5

Table 9 The intensity of the thulium emission at 450nm ($^1D_2 \rightarrow ^3H_4$), 475 nm ($^1G_4 \rightarrow ^3H_6$), 790 nm ($^3F_4 \rightarrow ^3H_6$) and 1600nm ($^3H_4 \rightarrow ^3H_6$) for Tm, Co, co-doped samples upon 675 nm excitation. The intensity of the sample without codopant is set to 100.

Dopant	I(450)	I(475)	I(790)	I(1600)	R(450/475)
Tm(0.2)	100±5	100±5	100±5	100±5	3.7±0.5
Tm(0.2)Co(0.1)	13±1	3±0.5	23±2	29±5	14±2
Tm(0.2)Co(0.5)	4.1±0.5	0.9±0.3	2.0±0.5	<5	14±3

Table 10. Specifications of recently reported upconversion (pumped) fiber

Authors and references	Allain et al. [61]	Allain et al. [87,90]	Millar et al. [95]
Dopant	Tm ³⁺	Ho ³⁺	Er ³⁺
Dopant concentration (ppm)	1250	1200	500
Glass type	ZBLAN	ZBLAN	ZBLAN
Core radius (μm)	1.5	1.35	4.5
Numeric aperture (NA)	0.14	0.16	0.10
Acceptance angle (degrees)	8.0	8.9	5.9
Temperature of operation (K)	77	300	300
Pump λ_p (nm)	647&676	647	801
Signal λ_s (nm)	455 (pulsed) 480 (spiked)	540-550 (CW)	850 (CW)
Threshold pump power (mW)	90 ^a	24 ^a	20 ^a
Coupling coefficient ρ	0.30	0.30	?
Slope efficiency	0.0057 ^c	0.36 ^c	0.38 ^d
Length of fiber (m)	1.7	0.45	3
Beam radius at λ_p (μm)	1.9	1.7	4.0
Beam radius at λ_s (μm)	1.5	1.5	4.1
Core area (μm^2)	7	6	64
Beam area at λ_p (μm^2)	11	9	50
Beam area at λ_s (μm^2)	7	7	53
V parameter at λ_p	2.0	2.0	3.6
V parameter at λ_s	2.9	2.4	3.4
$\lambda_{\text{cut-off}}$ at V = 2.4 (nm)	550	550	1200
Cavity	Tunable	Tunable	Tunable

lasers.

^a The quoted value is the injected pump power threshold, which is r times the input power of the pump laser.

- ^b The quoted value is the absorber power at the threshold.
^c Slope efficiency = D signal output power/D injected pump power.
^d Slope efficiency = D signal output power/D absorbed power.

CONCLUSION

In this paper we present properties of the active fluoride glasses. The high transparency within the wide range of the spectrum ($0.2\mu\text{m} - 7\mu\text{m}$) as well as the possibility for the easy incorporation of the trivalent lanthanides make these glasses good laser hosts. These characteristics, along with the refraction index near 1.5 and good resistance to degradation from water or weak acids make these materials, especially the glass so called ZBLAN, promising candidate for ultra-low-loss optical fibres.

Moreover, the relatively low phonon energies offer potential possibilities to obtain more radiation transitions in trivalent lanthanides energies in comparison with other glasses (for example silica glasses). Especially, promising are possible efficient transitions at $1.3\mu\text{m}$ for optical telecommunications systems and an efficient upconversion processes leading to the radiative transitions in the visible range of the light spectrum. The latter property offers possibility of the application to construction of the compact devices generated blue coherent radiation suited to high density optical recording.

REFERENCES

- [1] Poulain M., Poulain M. and Lucas J., *Mat.Res.Bull.* 10, 1974, 243.
- [2] Drexhage M.G., Moynihan C.T., Laleh Boulos M., and Quinlan K.P., in *Proceedings of the Conference on the Physics of Fiber Optics*, ed. by Bendow B. and Mitra S.S. Columbus, Ohio: American Society, 1981
- [3] France P.W., Drexhage M.G., Parker J.M., Moore M.W., Carter S.F. and Wright V., *Fluoride Glass Optical Fibres*, Blackie/CRC Press, 1990
- [4] Brieley M.C. and France P.W., *Electron. Lett.*, 1987, 23, 815
- [5] Lucas J., Chanthanasinh M., Poulain M., Poulian M., Brun P., and Weber M.J., *J.Non-Cryst.Solids*, 1978,27, 273
- [6] Reinfeld R., Greenberg E., Brown R.N., Drexhage M.G., and Jorgesen C.K., *Chem.Phys.Lett.* 95, 1983, 91

- [7] Reisfeld R., Katz G., Spector N., Jorgensen C.K., Jacoboni C., and DePape R., *J.Solid Chem.*, 41, 1982, 253
- [8] Reisfeld R., Katz G., Jacoboni C., DePape R., Drexhage M.G., Brown R.N. and Jorgensen C.K. *J.Solid Chem.*, 48, 1983 323
- [9] Shinn M.D., Sibley W.A., Drexhage M.G., and Brown R.N., *Phys.Rev.B* 27, 1983 6635
- [10] Cho W., Kim M.M., Jo J., Hahn T.: Lifetime variation of 4I13/2 level of E^{3+} in fluorozirconate glasses. Halide glasses VI, Clausthal, Germany 1989
- [11] Yanagita H., Okada K., Miura K., Toratani H., and Yamashita T.: E^{3+} fluoro-zirconate-aluminium glasses. Halide glasses VI, Clausthal, Germany 1989
- [12] Sanz J., Cases R., and Alcala R., *J.Non-Cryst.Solids* 93, 1987, 377
- [13] Guery C., Adam J.L., and Lucas J., *J.Lum.* 42, 1988, 181
- [14] Eyal M., Greenberg E., Reisfeld R., and Spector N., *Chem.Phys.Lett*, 117, 1985 108
- [15] Reisfeld R., Eyal M., Greenberg E., and Jorgensen C.K., *Chem.Phys.Lett*, 118, 1985, 25
- [16] Adam J.L., Guery C., Lucas J., Rubin J., Moine B., and Boulon G., *Mat. Sc. Forum* 19-20, 1987, 573
- [17] Pollack S.A. and Robinson M., *Electron. Lett.*, 24, 1988, 320
- [18] Auzel F., Meinchennin D., and Poignant H., *Electron. Lett.*, 24, 1988, 909
- [19] Brierley M.C. and France P.W., *Electron. Lett.*, 24, 1988, 935
- [20] Auzel F., Meichnenin D. and Poignant H., *Electron. Lett.*, 24, 1988, 1416
- [21] Quimby R.S. and Miniscalco W., *Appl.Opt.*, 28, 1989, 14
- [22] Allain J.Y., Monerie M., and Poignant H., *Electron. Lett.*, 25, 1989, 28
- [23] Allain J.Y., Monerie M., and Poignant H., *Electron. Lett.*, 25, 1989, 1082
- [24] Allen R., Esterowitz L., and Ginther R.J., *Appl.Phys.Lett.*, 56, 1990, 1635
- [25] Allain J.Y., Monerie M., and Poignant H., *Electron. Lett.*, 27, 1991, 445
- [26] Ronarc'h D., Guibert M., Auzel F., Mechenin D., Allain J.Y., and Poignant H., *Electron. Lett.*, 27, 1991, 511
- [27] Esterowitz L., Allen R., and Aggarwal I., *Electron. Lett.*, 24, 1988, 1104
- [28] Allain J.Y., Monerie M., and Poignant H., *Electron. Lett.*, 25, 1989, 1660
- [29] Carter J.N., Smart R.G., Hanna D.C., and Tropper A.C., *Electron. Lett.*, 26, 1990, 1759
- [30] Percival R.M., Carter S.F., Szebista D., Davey S.T., and Stallard W.A., *Electron. Lett.*, 27, 1991, 1912

- [31] Smart R.G., Tropper A.C., Hanna D.C., Carter J.N., Davey S.T., Carter S.F., and Szebista D., *Electron. Lett.*, 28, 1992, 58
- [32] Carter J.N., Smart R.G., Tropper A.C., and Hanna D.C., *J.Non-Cryst.Solids*, 140, 1992, 10
- [33] Allain J.Y., Monerie M. and Poignant H., *Electron. Lett.*, 27, 1991, 189
- [34] Ohishi Y., Terutoshi T., and Takahasi S., *IEEE Photo.Techno.Lett.*, 3, 1991, 688
- [35] Ohishi Y., Kanamori T., *Electron. Lett.*, 28, 1992, 162
- [36] Brieley M.C., France P.W., and Millar C.A., *Electron. Lett.*, 24, 1988, 539
- [37] Wetenkamp L., *Electron. Lett.*, 26 1990, 883
- [38] Allain J., Monerie M., and Poignant H., *Electron. Lett.*, 27, 1991, 1513
- [39] Smart R.G., Carter J.N., Tropper A.C., Hanna D.C., Carter S.F., and Szebista D. 10, 1991, 1702
- [40] Carter J.N., Smart R.G., Tropper A.C., Hanna D.C., Carter S.F., and Szebista D. *J.Lightwave Techn.*, 9, 1991, 1548
- [41] Ohoshi Y., Kanamori K., Kitagawa T., Takahashi S., and Snitzer E., *Opt.Lett.*, 16, 1991, 1747
- [42] Durteste Y., Monerie M., Allain J.Y., and Poignant H., *Electron. Lett.*, 27, 1991, 626
- [43] Carter S.F., Szebista D., Davey S.T., Wyatt R., Brierly M.C., and France P.W., *Electron. Lett.*, 27, 1991, 628
- [44] Allain J.Y., M.Monerie, and H.Poignat, *Electron. Lett.*, 27, 1991, 1012
- [45] Ohishi Y., Kanamori T., and Takahashi S., *IEEE Photo. Techn. Lett.*, 3, 1991, 715
- [46] Lobbet R., Wyatt R., Eardley P., Smyth P., Szebasta D., Carter S.F., S.T. Davey, C.A.Davey, and M.C.Brieley, *Electron. Lett.*, 27, 1991, 1472
- [47] Ohishi Y., Kanamori T., Temmyo J., Wada M., Yamada M., Shimizu M. Yoshino K., Hanafusa H., Horiguchi M., and Takahashi S., *Electron. Lett.*, 27, 1991, 1995
- [48] Ohishi Y., Kanamori T., Nishi T., Takahashi S., and Snitzer E., *IEEE Trans-Phot.on. Techn. Lett*, 3, 1991, 990
- [49] Miajima Y., Sugawa T., and Fukasaku Y., *Electron. Lett.*, 27, 1991, 1706
- [50] Obro M., Pedersen J.E., and Brieley M.C., *Electron. Lett.*, 28, 1992, 99
- [51] Ronarc'h D., Guibert M., Ibrahim H., Monerie M., Poignant H., and Tromeur A., *Electron. Lett.*, 27, 1991, 908

- [52] Witley T.J., Millar C.A., Brierly M.C. , and Carter S.F., *Electron. Lett.*, 27, 1991, 184
- [53] Zirngibl M., *Electron. Lett.*, 27, 1991, 560
- [54] Nakazawa M. and Kimura Y., *Electron. Lett.*, 27, 1991, 1065
- [55] Percival R.M., Cole S., Cooper D.M., Craig-Rayn S.P., Ellis A.D., Rowe C.J. and Stallard W.A., *Electron. Lett.*, 27, 1991, 1266
- [56] Pedersen B., Zemon S., and Miniscalco W.J., *Electron. Lett.*, 27, 1991, 1295
- [57] Townsend J.E., Barnes W.L., and Jędrzejewski K.P., *Electron. Lett.*, 27, 1991, 1958
- [58] Ohashi M. and Shiraki K., *Electron. Lett.*, 27, 1991, 2143
- [59] Horiguchi M., Shimizu M., Yamada M., Yoshino K., and Hanafusa H., *Electron. Lett.*, 27, 1991, 2319
- [60] Quimby R.S. , Drexhage M.G., and Suscavage M.J., *Electron. Lett.*, 23, 1987, 32
- [61] Allain J.Y., Monerie M., and Poignant H., *Electron. Lett.*, 26, 1990, 166
- [62] Allain J.Y., Monerie M., and Poignant H., *Electron. Lett.*, 27, 1991, 1156
- [63] Smart R.G., Hanna D.C., Tropper A.C., Davey S.T., Carter S.F., and Szebesta D., *Electron. Lett.*, 27, 1991, 1307
- [64] Whitley T.J., Millar C.A., Wyatt R., Brierly M.C., and Szebesta D., *Electron. Lett.*, 27, 1991, 1785
- [65] Hirao K., Tanabe S., Kishimoto S., Tamai K., and Soga N., *J.Non-Cryst. Solids*, 135, 1991, 90
- [66] Allain J.Y., Monerie M., and Poignant H., *Electron. Lett.*, 28, 1992, 111
- [67] Hirao K., Todoroki S., and Soga N., *J.Non-Cryst. Solids*, 143, 1992, 40
- [68] Poulain M., Chap.2, *Fluoride Glasses*, ed.A.E.Comyns, Wiley, 1989
- [69] Haixing Z. and Fuxi G., *Chinese Phys.*, 1986, 6, 978
- [70] Millar C.A., Fleming S.C., Brierley M.C., Hunt M.H., *IEEE Photon.Lett.*, 2 , 415, 1990
- [71] Davey S.T. and France P.W., *Brit. Telecom Technol. J. ,* 7, 1989, 58
- [72] Yamashita T., *Proc. SPIE*, 1171, 1989, 291
- [73] Tran D.C., Fsher C.F., and Sigel G.H., *Electron. Lett.*, 18, 1982, 657
- [74] Durteste Y., Monerie M., Allain J.Y.. , and Poignat H., *Electron. Lett.*, 27, 1991, 626
- [75] Carter S.F., Szebesta D., Davey S.T., Wyatt R., Brierley M.C., and France P., *Electron. Lett.*, 27 1991, 628

- [76] Auzel F., *Proc.IEEE*, 61, 1973, 758
- [77] Allain J.Y., Monerie M., and Poignant H., *Electron. Lett.*, 27, 1991, 1012
- [78] Ronarc,h D., Guibert M., Auzel F., Mechenin D., Allain J.Y., Poignat H., *Electron Lett.*, 27, 1991, 511
- [79] Perciyal R.M., Szebesta D., and Davey S.T., *Electron. Lett.*, 28, 1992, 671
- [80] Percival R.M., Szebesta D., Davey S.T., Swain N.A., and King T.A., *Electron.Lett.*, 28, 1992, 2231
- [81] Auzel A. and Pecile D., *J.Luminesc.*, 11, 1976, 321
- [82] Oomen E.W.J.L., le Gall P.M.T. , and van Dongen A.M.A. , *J.Luminesc.*, 46, 1990, 353
- [83] Reisfeld R., *Spectroscopy of Solid-State Laser-Type Materials*. New York: B.DiBartolo, Penum, 1987
- [84] Quimby R., Drexhage M.G., and Suscavage M.J., *Electron. Lett.*, 23, 1987, 32
- [85] Silversmith A., Lenth W., and Macfarlane R.M., *Appl.Phys.Lett.*, 45, 1987, 1977
- [86] Macfarlane R.M., *Appl.Phys.Lett.*, 54, 2301, *Appl.Phys.Lett.*, 45, 1989, 1977
- [87] Allain J.Y., Monerie M., and Poignant H., *Electron. Lett.*, 26, 1990, 261
- [88] Yeh D.C., Sibley W.A., and Suscavage M.J., *J.Appl.Phys.*, 63, 1988, 4644
- [89] Chamarro M.A. and Cases R., *J.Luminesc.*, 42, 1988, 267
- [90] Rich T.C. and Pinnow D.A., *J.Appl.Phys.*, 43, 1972, 2357
- [91] Monerie M., Georges T., Francois P.L., Allain J.Y., and Neveaux D., *Electron. Lett.*, 26, 1990, 320
- [92] Oomen E.W.J.L. and Lous E.J. , *Philips J.Res.*, 46, 1992, 157
- [93] *Optical Fibre Lasers and Amplifiers*
- [94] Miniscalco M.J., Andrewws L.J., Thomson B.A., Wei , and Hall B.T., *Proc. SPIE*, 1171, 1989
- [95] Millar C.A., Brierley M.C., Hunt M.H., and Carter S.F., *Electron.Lett.*, 26, 1990, 1871